The Journal of Immunology

T Cells Retain Pivotal Antitumoral Functions under Tumor-Treating Electric Fields

Gil Diamant, Hadar Simchony Goldman, Lital Gasri Plotnitsky, Marina Roitman, Tamar Shiloach, Anat Globerson-Levin, Zelig Eshhar, Oz Haim, Niv Pencovich, Rachel Grossman, Zvi Ram and Ilan Volovitz

J Immunol published online 2 July 2021
http://www.jimmunol.org/content/early/2021/07/02/jimmunol.2100100

Supplementary Material **http://www.jimmunol.org/content/suppl/2021/07/02/jimmunol.2100100.DCSupplemental**

The Journal of Immunology is published twice each month by The American Association of Immunologists, Inc., 1451 Rockville Pike, Suite 650, Rockville, MD 20852

Print ISSN: 0022-1767 Online ISSN: 1550-6606.

Published July 2, 2021, doi:10.4049/jimmunol.2100100

T Cells Retain Pivotal Antitumoral Functions under Tumor-Treating Electric Fields

Gil Diamant,*,†,[1] Hadar Simchony Goldman,*,[1] Lital Gasri Plotnitsky,* Marina Roitman,* Tamar Shiloach,‡ Anat Globerson-Levin,‡ Zelig Eshhar,‡ Oz Haim,† Niv Pencovich,† Rachel Grossman,† Zvi Ram,† and Ilan Volovitz*,†

Tumor-treating fields (TTFields) are a localized, antitumoral therapy using alternating electric fields, which impair cell proliferation. Combining TTFields with tumor immunotherapy constitutes a rational approach; however, it is currently unknown whether TTFields' locoregional effects are compatible with T cell functionality. Healthy donor PBMCs and viably dissociated human glioblastoma samples were cultured under either standard or TTFields conditions. Select pivotal T cell functions were measured by multiparametric flow cytometry. Cytotoxicity was evaluated using a chimeric Ag receptor (CAR)–T–based assay. Glioblastoma patient samples were acquired before and after standard chemoradiation or standard chemoradiation + TTFields treatment and examined by immunohistochemistry and by RNA sequencing. TTFields reduced the viability of proliferating T cells, but had little or no effect on the viability of nonproliferating T cells. The functionality of T cells cultured under TTFields was retained: they exhibited similar IFN-γ secretion, cytotoxic degranulation, and PD1 upregulation as controls with similar polyfunctional patterns. Glioblastoma Ag–specific T cells exhibited unaltered viability and functionality under TTFields. CAR-T cells cultured under TTFields exhibited similar cytotoxicity as controls toward their CAR target. Transcriptomic analysis of patients' glioblastoma samples revealed a significant shift in the TTFields-treated versus the standard-treated samples, from a protumoral to an antitumoral immune signature. Immunohistochemistry of samples before and after TTFields treatment showed no reduction in T cell infiltration. T cells were found to retain key antitumoral functions under TTFields settings. Our data provide a mechanistic insight and a rationale for ongoing and future clinical trials that combine TTFields with immunotherapy. ***The Journal of Immunology*****, 2021, 207: 1–11.**

Tumor-treating fields (TTFields) are a locoregional antitumoral treatment that uses alternating electric fields tuned to target proliferating cells. TTFields exert an electric torque on highly polar proteins cardinal to the mitotic phase of cell division, thereby disrupting mitotic spindle formation. These physical interactions result in inhibiting proliferation and inducing cancer cell death (1).

Optune is a medical TTFields delivery device that has demonstrated antimitotic effects in preclinical and clinical research on several solid tumors (2). Optune has been U.S. Food and Drug Administration–approved for treatment of recurrent and newly diagnosed glioblastoma (GBM), in which, when delivered concurrently with standard chemoradiation therapy, it was shown to significantly prolong progression-free and overall survival while maintaining good quality of life (3). It was recently approved also for the treatment of malignant pleural mesothelioma (4), and it is currently being tested in phase III clinical trials for ovarian (NCT03606590), pancreatic (NCT03377491), liver (NCT03606590), gastric (NCT04281576), and non–small-cell lung cancer (NCT02973789). Notwithstanding, even following a survival extension of 4.8 mo, the median survival of newly diagnosed GBM patients remains only 20.8 mo, highlighting the need for more effective multimodal treatments (5).

Cancer immunotherapy is a central arm in battling malignancies (6). Responses to immunotherapy frequently positively correlate with tumor neoantigen load, PDL1 expression and the abundance of tumor-infiltrating T lymphocytes (TILs) as found in immunologically "hot" tumors (7). Unfortunately, gliomas have low neoantigen load and are considered immunologically "cold" (8, 9), with the majority of patients failing to respond to immunotherapy (9, 10).

The immune system may play an important role in mediating the clinical effects of TTFields. TTFields was shown to reduce distant metastatic spread to the lungs in a rabbit renal cancer model and to enhance the peri- and intratumoral infiltration of $CD4^+$, $CD8^+$ T cells (11). It was shown to enhance antitumor efficacy when combined with anti-PD1 in mouse tumor models, plausibly by their induction of

*The Cancer Immunotherapy Laboratory, Neurosurgery Department, Tel-Aviv Medical Center, Sackler Faculty of Medicine, Tel-Aviv University Tel-Aviv, Israel; †Neurosurgery Department, Tel-Aviv Medical Center, Sackler Faculty of Medicine, Tel-Aviv University, Tel-Aviv, Israel; and ‡Laboratory for Cancer Research and Immunotherapy, Tel-Aviv Medical Center, Sackler Faculty of Medicine, Tel-Aviv University, Tel-Aviv, Israel

[1]G.D. and H.S.G. contributed equally to this work.

ORCIDs: 0000-0003-2052-0751 (H.S.G.) and 0000-0001-6343-8876 (M.R.).

Received for publication February 2, 2021. Accepted for publication April 28, 2021.

This work was supported by a grant from Novocure. The grant partially (I.V. and L.G.P.) or fully (G.D.) covered salary and travel assistance for presenting the results of this study. R.G. received an unrelated institutional grant from Novocure. Z.R. received an institutional grant from Novocure.

The RNA-Seq data presented in this article have been submitted to the European Genome-Phenome Archive (https://ega-archive.org/studies/EGAS00001005392) under accession number EGAS00001005392.

Conception and design: I.V., Z.R., R.G., G.D., H.S.G., L.G.P., and Z.E.; development of methodology: I.V., G.D., H.S.G., L.G.P., M.R., T.S., A.G.-L., and N.P.; conducting experiments: G.D., H.S.G., L.G.P., O.H., and N.P.; analyzing data: I.V., G.D., H.S.G., L.G.P., and M.R.; writing the manuscript: I.V., G.D., and H.S.G. All authors have read and approved the final manuscript.

Address correspondence and reprint requests to Dr. Ilan Volovitz or Dr. Zvi Ram, Tel-Aviv Medical Center, 6 Weizmann St. Tel-Aviv 6423906, Israel. E-mail addresses: ilanv@tlvmc.gov.il (I.V.) or zviram@tlvmc.gov.il (Z.R.)

The online version of this article contains supplemental material.

Abbreviations used in this article: GBM, glioblastoma; ICD, immunogenic cell death; IHC, immunohistochemical; RNA-Seq, RNA-sequencing; TAST, tumor Ag–specific T cell; TIL, tumor-infiltrating T lymphocyte; TTField, tumor-treating field.

immunogenic cell death (ICD) in tumor cells (12–14). In a retrospective study in GBM patients, the overall survival benefit of TTFields was found to correlate with higher blood T cell counts and with low (<4.1 mg) or no administration of immunosuppressive dexamethasone (15). Of note, being a locoregional physical treatment, TTFields is likely to cause minimal or no systemic immunosuppression. Several early phase trials combining TTFields with checkpoint inhibitors (CPIs) (NCT02973789, NCT03405792, NCT03903640, NCT03 430791) or other immunotherapeutics (NCT03223103) are underway. However, the direct effects of TTFields on T cells, the main drivers of antitumoral responses are unknown. Understanding the extent to which T cells generate an immune response under the locoregional effects of TTFields is therefore of key mechanistic importance to current and future trials combining immunotherapy with TTFields.

In this study, we employed the inovitro system, enabling application of TTFields on cultured cells, to evaluate the effect of TTFields on T cells. We examined TTFields' effects on T cell proliferation, viability, and select pivotal antitumoral functions using healthy donor PBMCs and TILs from resected GBM samples. We evaluated direct cytotoxicity using a CAR-T cell–based system. We also performed immunohistochemical (IHC) analysis and comparative transcriptomic evaluation on GBM samples obtained from patients before and after TTFields treatment to assess TTFields' treatment effects on T cell infiltration and on broad immune gene expression.

Materials and Methods

Cells, tissue culture, and patients'/donors' samples

PBMC were produced from leukocyte-enriched fractions from healthy blood donations obtained from the Israeli blood bank. All tissue culture was performed in X-VIVO15 serum-free defined medium (Lonza Pharma and Biotech, Basel, Switzerland) supplemented with 1:5000 Benzonase (Novagen, Billerica, MA) to gently dissociate DNA and RNA split from dead cells.

Human GBM viable single-cell suspensions were produced by dissociating tumor samples using neutral protease from *Clostridium histolyticum* (AMSBio, Abingdon, UK) (16). The dissociated tumor cells were freshly assayed. Healthy donor blood and patients' GBM samples were received under institutional ethical approval (0408-10-TLV). Samples were received from patients signing an informed consent.

CAG multiple myeloma cells were obtained from the American Type Culture Collection (Manassas, VA) and maintained in RPMI 1640 (Life Technologies, Grand Island, NY), 10% FBS, 1% sodium pyruvate, 1% glutamine and penicillin/streptomycin (Biological Industries, Beit Haemek, Israel). HER2-expressing CAG cells were generated by transfection (jetPRIME; Polyplus-transfection, Illkirch-Graffenstaden, France) with human HER2 and G418 resistance genes. HER2-CAG cells were cultured in the CAG medium containing 0.5 mg/ml G418 (Life Technologies). T cells expressing an anti-HER2 CAR were generated by retroviral transduction of healthy donor PBMC samples with a vector encoding the N29 anti-Her2 CAR and GFP [see (17)].

Institutional ethical approval was received for use of blood donations and GBM samples (0408-10-TLV). Samples were received from patients signing an informed consent. All authors all coauthors approve this submission. All data and materials are available upon request.

TTFields application in vitro

Cell culturing under TTFields conditions was conducted using the inovitro TTFields system (18) according to manufacturer's instructions unless described otherwise. Cells were seeded in the inovitro culture dishes and incubated either on baseplates generating an electric field within a heating/cooling incubator (Binder, Tuttlingen, Germany) or in a standard incubator. In vitro application of TTFields accelerated the evaporation of water from the media, thus distilled water was replenished daily in all plates. The electric parameters used in all assays matched those used in the clinic. Field frequency was set to 200 kHz (and also to 150 kHz in Supplemental Fig. 3), and field intensity was set at 2–2.5 V/cm (peak-to-peak), which is within the range found to optimally inhibit GBM cell growth (19) and as used in GBM patients.

Flow cytometry

Multicolor flow cytometric sample analysis was performed using a Canto-II Flow Cytometer (BD Biosciences, Franklin Lakes, NJ). Staining was performed in the dark and at room temperature. Abs used were as follows: CD3, CD4, and CD19 from eBioscience (San Diego, CA), CD107a, CD14, PD1, and IFN-γ from BioLegend (San Diego, CA) and CD8a from BD Biosciences. Data analysis was performed using FlowJo (Ashland, OR).

For CFSE staining, PBMC or GBM cell suspensions (1×10^7 to 5×10^7 cells per milliliter) were stained with CFSE (Thermo Fisher Scientific, Waltham, MA) 2 μM CFSE and 1.25% FCS 10 min, room temperature. The cells were then washed twice with PBS, 2.5% FCS, counted using trypan blue (Sigma-Aldrich, St. Louis, MO) and used for subsequent assays.

Viability assay

CFSE-stained PBMCs (3×10^6 cells per dish) were seeded in inovitro dishes, and either stimulated with 1% PHA (Life Technologies) or left untreated. The cells were incubated for 3.5 d under either TTFields or standard culture conditions. Cells were then harvested, stained for viability using violet fixable LIVE/DEAD amine viability dye (ViViD-L34955; Thermo Fisher Scientific) and then extracellularly for CD8a, CD14, and CD19. CD3 and CD4 were stained intracellularly using the Fix/Perm Kit (BD Biosciences) (20) as T cell activation drives their internalization. Cells were fixed with 1% formaldehyde (Electron Microscopy Sciences, Hatfield, PA) and analyzed by flow cytometry.

To enable inclusion of dead cells in this assay, autofluorescent debris (particles with medium-to-high signals on all channels that can be mistaken for dead cells) were gated out based on a higher CFSE signal and a lower side-scatter compared with T cells. Viability rates were calculated as live/total cells. The cells were categorized as live ($ViViD^{low}$) or dead ($ViViD^{high}$), and as proliferating ($CFSE^{low}$) or nonproliferating ($CFSE^{high}$).

T cell activation and polyfunctionality assays

CFSE-stained PBMC (3×10^6) or dissociated single cells from GBM samples were cultured as described above. Five hours before harvesting, the cultures was supplemented with fluorochrome-conjugated CD107a Ab, 0.07% Golgistop (BD Biosciences) and 0.1% brefeldin A (Sigma-Aldrich). Cells were collected, stained for viability, then stained extracellularly for CD8a, CD14, CD19, and PD1, and intracellularly for CD3, CD4, and IFN-γ.

In vitro cytotoxicity assay

Target cells (CAG-HER2 or CAG) and effector anti-HER2 human CAR-T cells were cocultured for 8 h at varying effector/target ratios in standard or TTFields culture conditions. Dishes were supplemented with 1:5000 Benzonase to reduce split DNA/RNA-related clumping. Cultures were stained with CD3, CD138 (a myeloma marker), and propidium iodide, staining dead cells (Sigma-Aldrich), and then analyzed by flow cytometry. Cell death rates in "target-only" were subtracted from those in matching "effector/target." The unspecific killing of parental CAG (non-HER2) was subtracted from its corresponding CAG-Her2 sample.

Statistical analysis

In vitro quantitative data are presented as mean ± SE. Statistical significance was determined by paired, two-tailed Student's *t* test and noted where significant (*$p < 0.05$, **$p < 0.005$). All in vitro experiments were repeated at least three times.

Tissue immunohistochemistry and cell frequency analysis

Tumor samples were obtained from four GBM patients before and after TTFields treatment (patient data in Supplemental Table STI). Tissue slides were immunohistochemically stained by hospital pathology services for CD3, CD4, and CD8 by the DAB-staining procedure. Tissue slides were scanned and then analyzed with the Aperio Imagescope program. Stained (i.e., brown-colored) nucleated cells (i.e., blue center) were counted in 4–6 representative 0.4 mm^2 fields in each slide. The cell counts were then averaged and normalized to cells per millimeter squared.

Tissue processing for RNA sequencing and library construction

Paired tumor tissues from 12 newly diagnosed GBM patients were obtained before and after treatment with standard chemoradiation (six controls) or with TTFields + chemoradiation (six TTFields). Processing and RNA extraction were performed with the PerfectPure RNA Tissue Kit (5 prime, Hilden, Germany). Illumina TruSeq RNA Library Prep v2 was used for sample preparation, generating mRNA-based libraries from total RNA input. Indexed samples were sequenced, in single-read mode, using the Illumina HiSeq 2500.

Transcriptomic analysis

RNA-sequencing (RNA-Seq) data were analyzed with DESeq2 software (21). Differential gene expression was compared on a broad list of 712 immune-related genes using the reads per kilobase million values. Statistical

analysis was performed using the negative binomial generalized linear model. Differences in expression before and after treatments were calculated per patient, and then averaged as net treatment effect per group. Fold-changes of net treatment effects (average of TTFields group over average of control group) were defined as significant when above 2 or below 0.5, with a Benjamini–Hochberg multiple comparison–corrected $p < 0.1$. The protumoral/antitumoral/mixed activity of each significantly altered gene was determined using published literature. The list of 712 genes related to immune activity was compiled using the Nanostring "nCounter PanCancer immune profiling panel" and the Thermo Fisher Scientific "Oncomine immune response" gene lists and the general literature. The list surveys all chemokines, cytokines and their receptors, transcription factors, immune checkpoint–related molecules, and other immune-related genes. The significance of the association (contingency) between protumoral to antitumoral genes (defined by the literature) significantly up or downregulated by TTFields- or by standardly treated patients was calculated using the Fisher exact method.

Results

TTFields reduce the viability of proliferating T cells

TTFields exert a cytostatic and cytotoxic effect on proliferating tumor cells. To evaluate T cell viability under TTFields, PBMCs were stained with CFSE and stimulated with PHA to induce proliferation. PHA was selected because of its TCR-dependent activation that simulates physiological activation requiring signal transduction, organelle redistribution, and actin cytoskeletal dynamics (22). Note that PHA stimulation is robust, leading to some activation-induced cell death. This affects both cell numbers and the viability rates. Cell doublets, B cells, monocytes, and autofluorescent debris were gated out and then $CD4^+$ and $CD8^+$ T cells were monitored for their proliferation status and viability (Fig. 1A).

No proliferation was detected in the PHA-nonstimulated samples. The number of cells in the nonstimulated TTFields-treated samples was lower by ∼15% to standardly incubated controls (Fig. 1B, left, $p = 0.01$) with no change in viability rates between groups (both 98%). This suggests that TTFields have a small to negligible effect on the number and the viability of nonstimulated T cells.

PHA stimulation drove some of the T cells to proliferate and affected both cell numbers and viability. The numbers of PHA-stimulated nonproliferating ($CFSE^{high}$) T cells in the TTFields-cultured samples was ∼35% lower than controls ($p = 0.015$ and $p = 0.03$ for $CD4^+$ and $CD8^+$ cells, respectively); however, their viability rates remained unaltered (Fig. 1B, right). In the same samples, the number of PHA-stimulated, proliferating ($CFSE^{low}$) T cells in the TTFields-cultured samples was lower by ∼75% to controls ($p = 0.009$ and $p = 0.01$ for $CD4^+$ and $CD8^+$, respectively) along with a decline in the viability rates, especially for the $CD8^+$ T cells (52% in the controls versus 40% in TTFields). These results align with TTFields' mechanism of action, i.e., marked inhibition and cytotoxic effect on proliferating cells with low impact on nonproliferating cells (23).

Key antitumoral functions in PHA-stimulated blood T cells are unaffected by TTFields

Many immune-related cellular processes such as secretion, degranulation, and surface molecule mobilization rely on cytoskeletal dynamics or on vesicular transport that may conceivably be

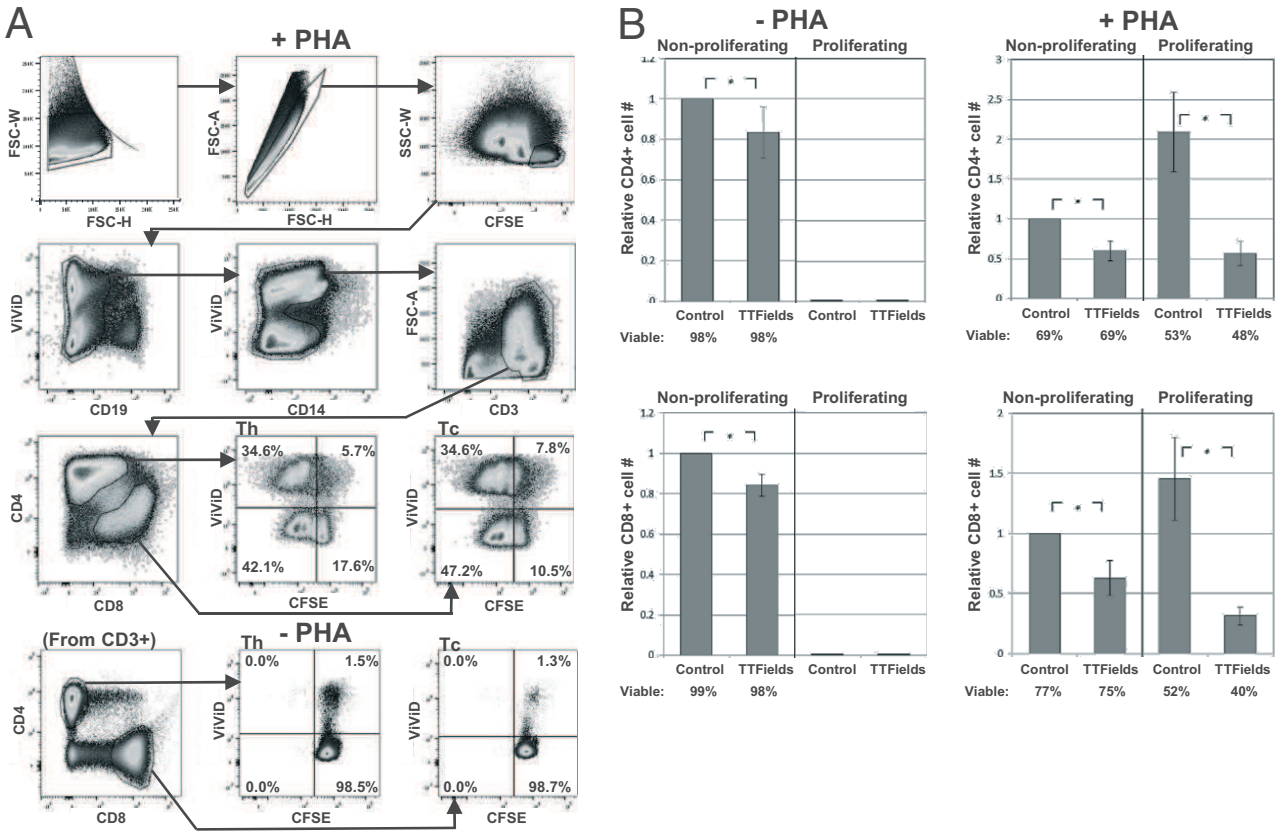

FIGURE 1. Effects of TTFields on the viability of peripheral blood T cells. CFSE-stained healthy donor PBMC were treated with PHA or left untreated and incubated under TTFields or standard conditions for 3.5 d. (**A**) Representative flow cytometric gating strategy for PHA-stimulated cells (top three rows) and partial gating for nonstimulated T cells. $CD4^+8^-$ Th cells or $CD8^+4^-$ CTL were divided into four groups according to viability (ViViD) and proliferation (CFSE) status. (**B**) Relative T cell numbers and viability rates in PHA-stimulated and nonstimulated samples, according to proliferative status. Data were normalized by setting the value of live, nonproliferating cells in control samples to one in each repeat. Stacked bars show normalized numbers of live cells. Viability rates (no. live / no. total) appear under each bar. Graphs show the mean of eight independent repeats using PBMC from four different donors tested during four separate experiments (two samples tested per donor in separate experiments). *$p < 0.05$.

perturbed by TTFields. To investigate whether key antitumoral functions are affected by TTFields, we simultaneously monitored proliferation (CFSE), activation/exhaustion (PD1), IFN-γ secretion and degranulation of cytotoxic granules [CD107a (24)] at single-cell resolution.

Gating identified $CD4^+$ and $CD8^+$ T cells, alongside $CD3^+CD14^-CD19^-CD4^-CD8^-$ cells, the majority of which are γδ-T cells (not shown) (Fig. 2A). We found that TTFields reduced to approximately half (but did not abolish) the fraction of proliferating $CD4^+$ or $CD8^+$ T cells. Importantly all other evaluated antitumoral functions were virtually unchanged between TTFields and standard PBMC cultures (Fig. 2B).

An key feature associated with effective responses to pathogens or tumors is the ability of individual activated T cells to respond by several concurrent functions, also known as polyfunctionality (25). A polyfunctionality analysis of T cells was performed on the dataset

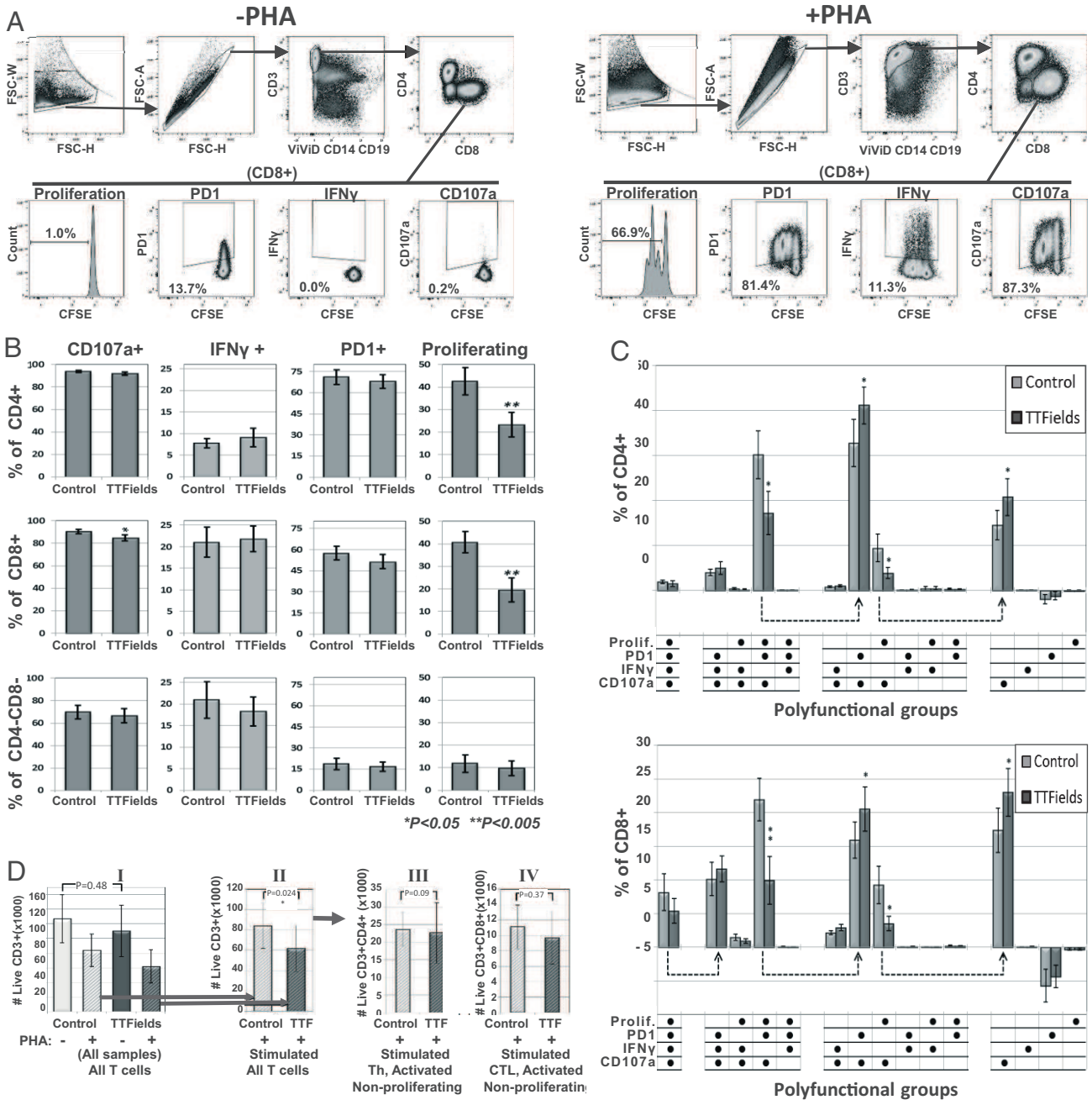

FIGURE 2. Effects of TTFields on the activation of blood-borne T cells. CFSE-stained donor PBMC were treated with PHA or left untreated and incubated under TTFields or standard conditions for 3.5 d. (**A**) Representative gating strategy for $CD3^+8^+4^-$ (CTL) evaluated for surface expression of PD1 and CD107a, for CFSE dilution and for IFN-γ production. Similar gating was performed for $CD3^+4^+8^-$ (Th) and $CD3^+4^-8^-$ T cells (the majority of which are γδ-T cells in healthy donor blood) (**B**–**D**) Net activation per function was calculated by subtracting the percent of positive cells in nonstimulated samples from the percent in matched PHA-stimulated samples. Graphs show the mean of 9–11 independent repeats using PBMC from six different donors tested over seven separate experiments. (B) Summary of functional responses grouped per single function. (C) Summary of polyfunctional analysis. Cells were divided into 15 mutually exclusive functional groups according to expression of one or more functions. Net percentage of polyfunctional-positive cells is presented. (D) Analysis of T cell viability in activated cells. Total number of live T cells in all samples (**I**) and in PHA-stimulated samples only (**II**). Graphs (**III**) and (**IV**) Cell numbers of activated nonproliferating cells (negative for proliferation but positive one of more other functions) in $CD4^+$ and $CD8^+$ T cells, respectively. $*p < 0.05$, $**p < 0.005$.

presented in Fig. 2B showing that, with the exception of proliferation, activated $CD4^+$ and $CD8^+$ T cells exhibited similar polyfunctional patterns under TTFields as under standard culture conditions (Fig. 2C). The data illustrate shifts of T cells from parallel polyfunctional groups that differed only in proliferation (e.g., from proliferating $PD1^+CD107^+$ to nonproliferating $PD1^+CD107^+$ cells). This may reflect relative shifts in fractions where part of the proliferating cells die, increasing the relative fraction of similarly activated but nonproliferating cells. These findings also demonstrate that proliferation is independent of other key antitumoral T cell functions, as previously shown by others (26). Although CD107a is not a standard Th marker, activated $CD4^+$ T cells have been shown to upregulate CD107a and secrete granzyme B (27). $CD4^+CD107^+$ T cells were reported to exhibit enhanced survival compared with their $CD4^+CD107a^-$ counterparts (28).

The above multiparametric dataset also enabled absolute enumeration of live cells according to cell type (CD4/8) and to proliferative status. Similar to the findings in Fig. 1, the number of live T cells found in nonstimulated samples cultured under TTFields was 85% that of controls (nonsignificant, $p = 0.48$) (Fig. 2DI). As in Fig 1B, the PHA-stimulated cultures contained significantly fewer T cells ($p = 0.024$) compared with standard-cultured conditions (Fig. 2DII). Importantly, there was no significant difference in the number of cells in these cultures when counting only the T cells which exhibited one or more activation parameters ("activated") other than proliferation (Fig. 2DIII, 2DIV, $CD4^+$ $p = 0.85$, $CD8^+$ $p = 0.37$). These results indicate that TTFields neither reduce the viability/number nor the functional responses in activated nonproliferating T cells. Note that the group of PHA-stimulated, activated but nonproliferating cells that was evaluated in Fig. 2D is a subgroup of the PHA-stimulated, nonproliferating cells evaluated in Fig. 1B.

Key antitumoral functions in GBM TILs are unaffected by TTFields

When compared with blood-borne T cells, TILs frequently distribute differently between memory/effector subsets and exhibit different effector and proliferation capacities (26, 29). The GBM microenvironment modifies T cell phenotypes (6), and TILs may thus respond differently than PBMC to TTFields. To examine the function of GBM TILs under TTFields conditions, viably dissociated (16) human GBM samples were incubated under standard or TTFields conditions (gating in Supplemental Fig. 1A). As with PBMCs, TIL proliferation was inhibited but not fully abolished under TTFields, whereas all other evaluated antitumoral T cell functions were unaffected (Fig. 3A). Upon PHA stimulation, TILs exhibited comparable polyfunctional responses under TTFields as under standard culture conditions (Fig. 3B).

Because the considerable heterogeneity in TIL frequencies among the different GBM samples, comparative cell enumeration (as in Fig. 2D) was not applicable. A more limited analysis of the relative fractions of live TILs was performed (Supplemental Fig. 1B) revealing no significant differences between control and TTFields-cultured GBM samples in the fraction of activated TILs responding to PHA stimulation by one or more functions other than proliferation (as in Fig. 2D). In the current study, stimulation of tumor-derived T cells under TTFields conditions was not performed under in vivo conditions (e.g., using rodent models), but rather under fresh, ex vivo conditions.

Notably, TIL enzymatic dissociation from tumor samples could potentially affect the functionality of TILs. Notwithstanding, the gentle dissociation methodology used in this study (16) together with the strong functional responses observed in the PHA-stimulated conditions suggest that the assayed TILs remained functionally intact.

Tumor Ag–specific T cells exposed to TTFields exhibit unaltered viability and function

TTFields are not expected to negatively affect tumor Ag–specific T cell (TAST) proliferation in tumor-draining lymph nodes located outside the treated field. However, TASTs may also proliferate within tumors (30) where TTFields may have an effect. To date, there are no unequivocal methods to identify which TILs constitute TASTs. However, Ahmadzadeh et al. (31) and Donia et al. (32) independently showed that the overwhelming majority of TASTs expresses PD1 on their surface. We relied on this characterization to evaluate the effect of TTFields on intratumoral TASTs by analyzing $PD1^+$ TILs in GBM cultures incubated without PHA stimulation under standard or TTFields conditions. Note that the rate of $PD1^+$ T cells within GBM TILs was considerably higher than the rate of $PD1^+$ T cells in the matching patients' PBMC (25% versus 3% in $CD8^+$, and 27% versus 7% in $CD4^+$ T cells, respectively; Supplemental Fig. 1A). This reflects local activation and/or exhaustion of some TILs (31). Importantly, we found that nonstimulated $PD1^+$ TASTs under TTFields or standard culture conditions exhibited similar baseline mono- and polyfunctionally (Fig. 3C).

Cytotoxic capacity of CAR-T cells is unaffected by TTFields

T cell–mediated cytotoxicity depends on the formation of a functional cytotoxic synapse. This requires extensive microtubule and centrosome realignment, which may plausibly be disrupted by TTFields (33). Given the importance cytotoxicity for effective immunotherapy and that our above findings on degranulation (CD107a) relate to a surrogate cytotoxicity marker, we directly assessed cytotoxicity under TTFields conditions using a CAR-T cell–based assay. CAR-T cells rely on the same intracellular machinery and processes as nonengineered T cells, supporting our choice of assay (34). In consideration that CAR-T cells are currently under clinical evaluation for GBM and other solid tumors (35), this assay also provides a general evaluation of possible compatibility of CAR-T cells with TTFields.

Human anti-HER2 CAR-T cells were cocultured with target cells, either parental (unaltered) CAG human myeloma cell line or CAG, which ectopically expresses HER2 (Fig. 4A). Target cell killing by HER2-specific CAR-T cells was unaffected by TTFields (Fig. 4B). Alternative gating of the same dataset examining the effector cells confirmed that TTFields had no effect on the viability of CAR-T effectors during the course of the assay (not shown). Taken together, these results demonstrate that TTFields do not interfere with T cell–mediated cytotoxicity.

Evaluating the clinical compatibility of TTFields with antitumoral immunity

To support our in vitro findings, we sought to examine the effect of TTFields on the immune response in clinical settings. First, we compared T cell infiltration rates in GBM samples resected before and after TTFields treatment from four patients by performing IHC staining for CD3, CD4, or CD8 (patient details in Supplemental Table STI). Although following TTFields treatment one patient's $CD3^+$ and $CD8^+$ TIL counts were slightly reduced, the infiltration rates in the other monitored patients were either unchanged (one patient) or strongly increased (two patients) (Fig. 5A). The representative images from one patient in Fig. 5B demonstrate that TTFields may accommodate, in some cases, large increase in TIL density. Obtaining paired before-after tissue blocks of samples was confined to a small number of tissue blocks we were able to recover and was limited only to patients receiving chemoradiation + TTFields, not to those receiving chemoradiation only. Nonetheless, the data demonstrate that TTFields application in patients does not preclude T

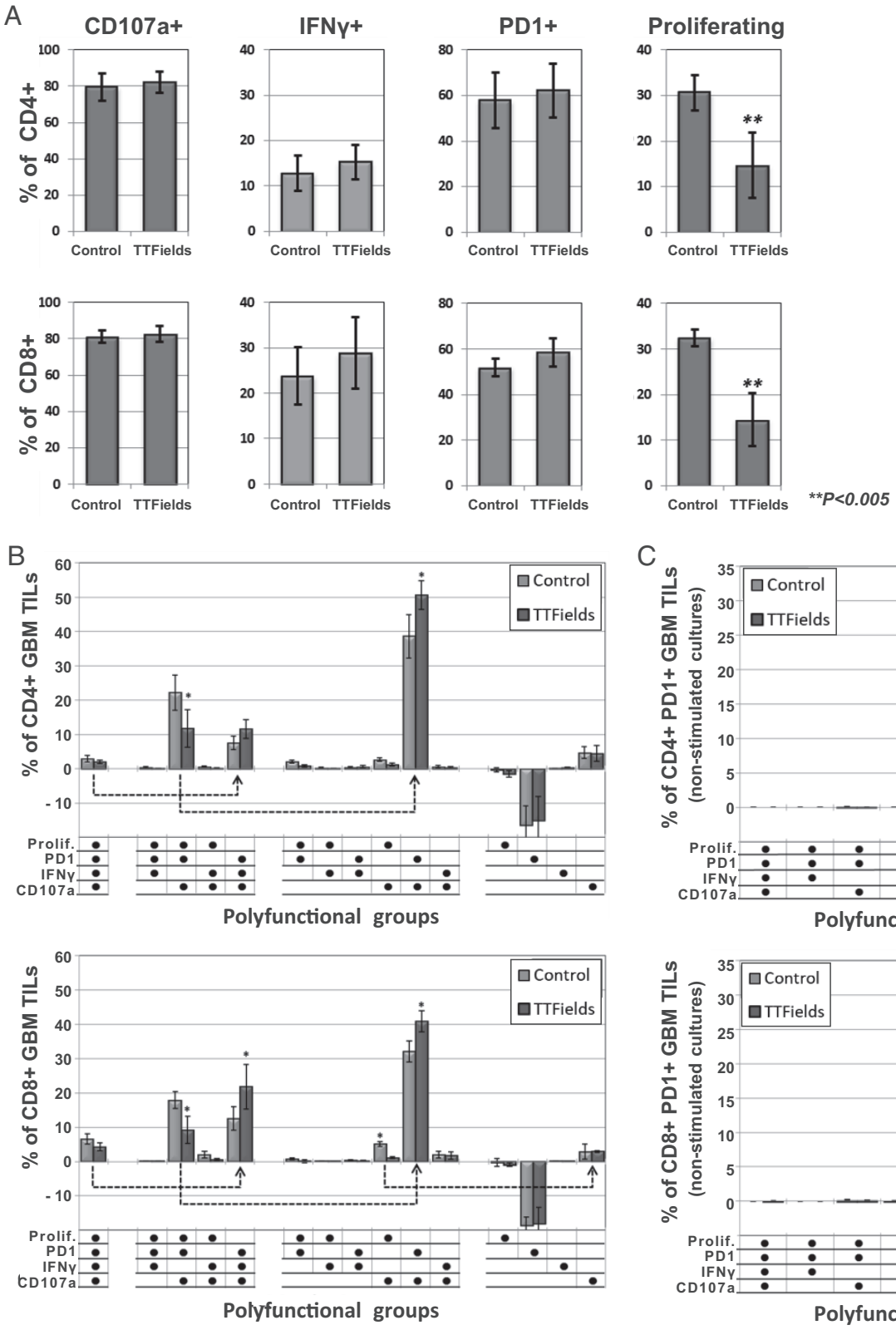

FIGURE 3. Effect of TTFields on activation of human GBM TILs. Fresh GBM samples were enzymatically dissociated to viable single cells, stained with CFSE, stimulated by PHA, or left untreated, and incubated under TTFields or standard conditions for 3.5 d. Cells were harvested and stained as described in Fig. 2. See gating in Supplemental Fig. 1A. PBMC samples were treated identically and used as guides for gating of data (not shown). Net activation was calculated by subtracting percent of positive cells in nonstimulated samples from percent in matched PHA-stimulated sample. Graphs show means and SE of three independent repeats with samples from three different GBM patients. (**A**) Summary of specific functional responses in $CD4^+$ and $CD8^+$ T cells. (**B**) Summary of polyfunctional analysis. Cells were divided into 15 mutually exclusive functional groups according to expression of one or more functions. Net percent of polyfunctional-positive cells is presented. (**C**) Relative rates and polyfunctionality of $PD1^+$ TILs (TASTs) in the nonstimulated samples. The $PD1^+$ T cells were divided into eight distinct polyfunctional groups according to their expression of one or more functions. $*p < 0.05$, $**p < 0.005$.

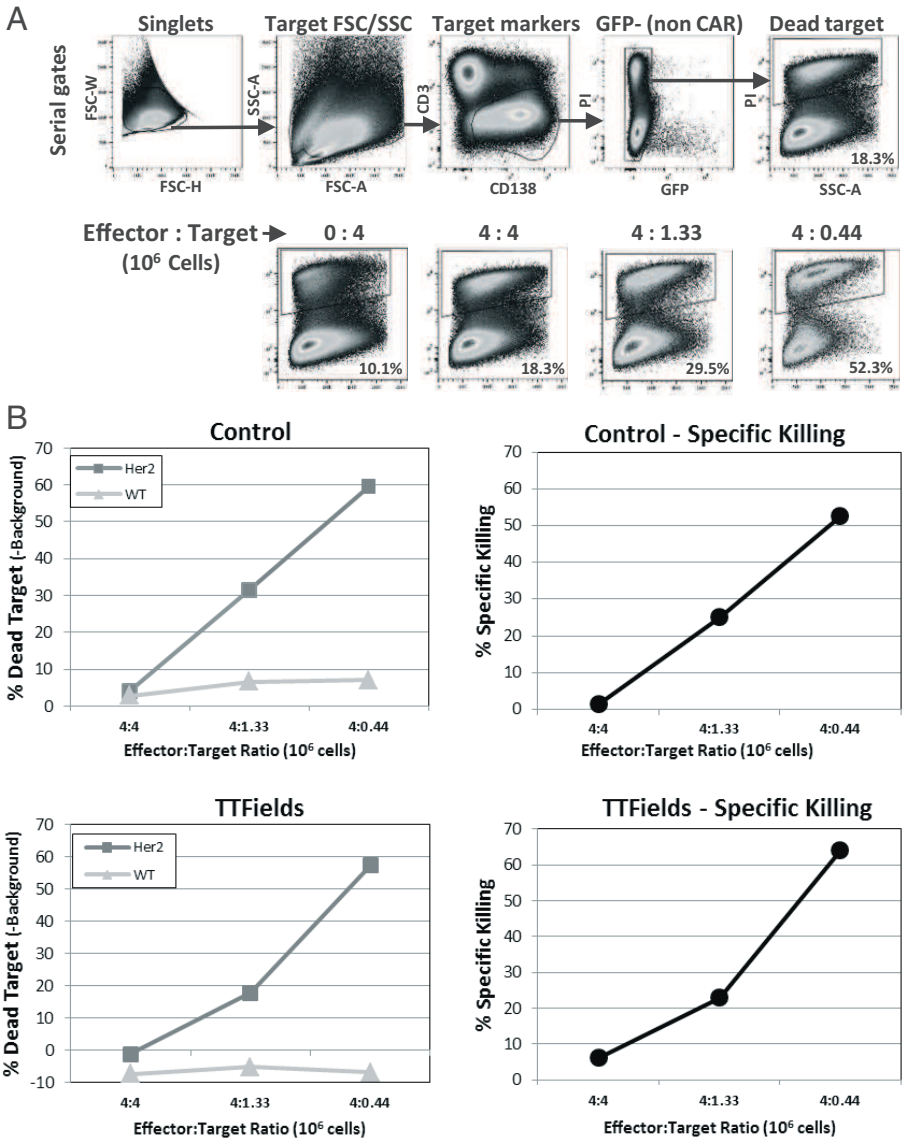

FIGURE 4. Effect of TTFields on direct cytotoxicity of CAR-T cells. Effector human anti-HER2 CAR-T cells and target cells expressing HER2 (CAG-Her2) or not expressing it (CAG) were cocultured under TTFields or control conditions for 8 h. Target cells were also cultured alone to determine background cell death. (**A**) Top row, Representative gating strategy. Bottom row, Dot plots displaying the viability for all four effector/target ratios tested. (**B**) Specific killing curves. The dead cell fraction in "target only" samples was subtracted from the concordant samples (lighter versus darker lines, respectively). Net specific killing (black line) was calculated by subtracting the fraction of killed cells in the CAG samples from that in the CAG-HER2 samples. Representative results (CAR transduction efficiency ≈ 35%) from one assay are shown. Similar results were observed in three independent repeats. Averages not presented because of markedly varying killing rates among donors, stemming from differences in and CAR transduction efficiencies and donor cells cytotoxic potency.

cells infiltration into tumors and that in some cases, TIL frequencies had significantly increased under treatment.

We next evaluated how TTFields modulate immune activity within GBM tissues by transcriptomic analysis. GBM samples were obtained before and after treatment of six patients treated by standard chemoradiation protocol (controls) and six patients treated by chemoradiation and TTFields (patient details in Supplemental Table STI). Differential gene expression analyses (Supplemental Fig. 2) demonstrated similar T cell infiltration trends as found in the IHC (Fig. 5). Specifically, the net post- minus pretreatment expression levels of the CD3, CD4, and CD8 genes (representative of T cell infiltration) were slightly higher in the TTFields group than in the control group, both per individual patients and per the averaged group. Although transcriptomic signatures are not as definitive as IHC to evaluate infiltration, it nevertheless supports our IHC data using an additional set of 12 before/after samples.

We next evaluated the effect of TTFields on the expression of a comprehensive set of 712 immune-related genes. The table in Fig. 5C summarizes all genes within this gene set found to be significantly up- or downregulated in either group. Genes were classified as having protumoral, antitumoral, mixed, or unknown roles based on published literature.

Overall, the data demonstrated a significant shift in the immune-related gene expression from protumoral to antitumoral signature following TTFields + chemoradiation treatment compared with treatment by chemoradiation alone ($p = 0.026$ Fisher exact). Notably, the antitumoral genes that were upregulated by TTFields' included granulysin, a key cytotoxic molecule, NKG2D (an NK activator receptor associated with TTFields-induced NK killing of glioma cells) (36) and *t*-bet (a hallmark Th_1 transcription factor). TTFields' treatment downregulated protumoral genes including IL18 (a proinflammatory cytokine), CXCL14 (a chemokine driving a suppressive tumor microenvironment), PDL2 (related to T cell exhaustion), and IL4 and IL17RB, which polarize Th to ineffective or protumoral functions.

Discussion

Knowing the effect of TTFields on T cells is critical when considering the pivotal role of T cells in antitumoral immune responses. By evaluating key antitumoral T cell functions ex vivo, our findings (Figs. 1, 2, and 3) indicate that TTFields operated at established therapy-relevant conditions do not hinder key T cell functions aside from proliferation. Our findings hold not only to cells derived from healthy donor blood but also to GBM TILs. Cytotoxicity is also not impeded by TTFields as shown by a CAR-T cell–based assay. To our knowledge, our

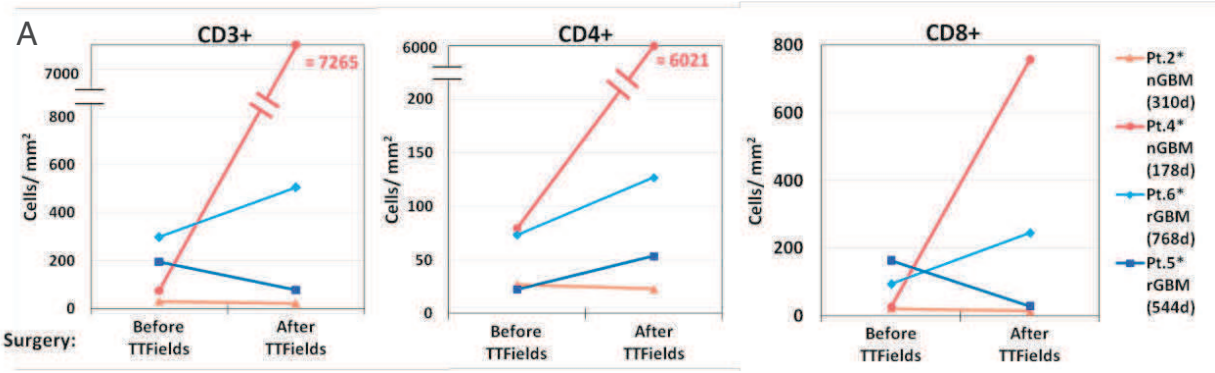

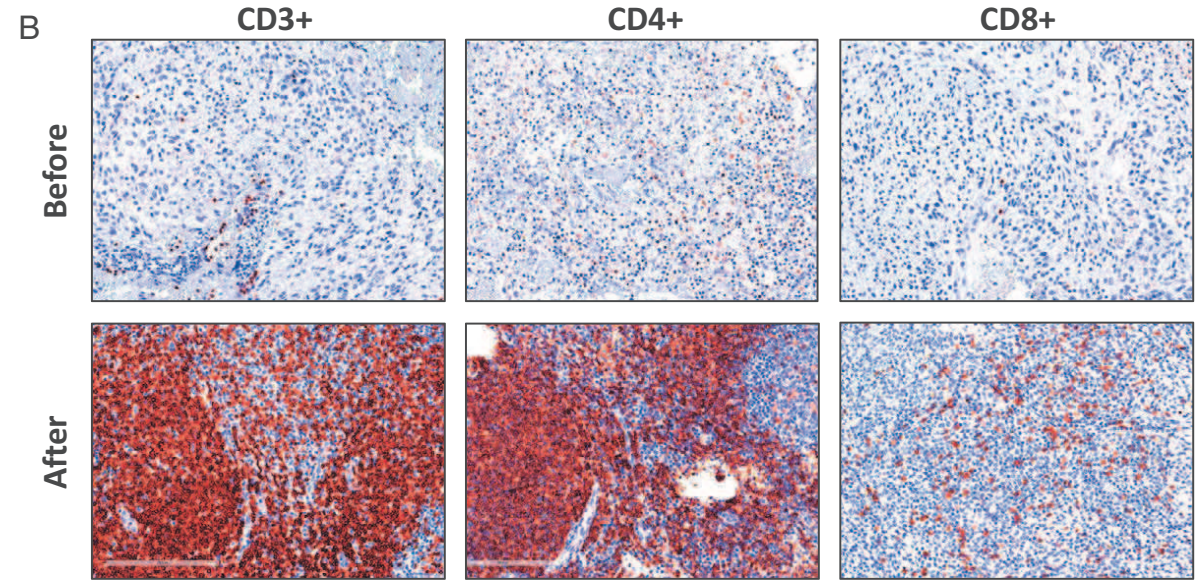

C

Upregulated after TTFields

Gene	Fold change	F.D.R P-val'	Effect on tumors
IL11	8.5	0.001	Mixed
GPR18	5.9	0.071	Unknown
CD70	5	0.079	Mixed
CCL26	4.5	0.031	Pro
NKG2D	4.2	0.034	Anti
T-bet	3.4	0.019	Anti
ICOS-L	3.3	0.094	Anti
ISG15	3.2	0.035	Anti
Fac. XII	3.1	0.032	Unknown
HGF	3	0.041	Pro
GNLY	2.6	0.083	Anti
MMP2	2.5	0.036	Pro

Downregulated after TTFields

Gene	Fold change	F.D.R P-val'	Effect on tumors
IL36B	0.1	0.013	Pro
C4BPA	0.11	0.026	Unknown
IL4	0.12	0.004	Pro
C7	0.21	0.098	Pro
CXCL14	0.22	0.093	Pro
IFNE	0.23	0.038	Unknown
MPL	0.25	0.097	Pro
IRF6	0.28	0.09	Anti
TSLP	0.29	0.005	Pro
DMBT1	0.3	0.087	Mixed
GPR75	0.32	0.022	Unknown
AKR2	0.32	0.027	Anti
PDL2	0.35	0.013	Pro
TNFSF11 B	0.35	0.026	Pro
IL17RB	0.41	0.004	Pro
NAMPT	0.41	0.098	Pro
LIFR	0.44	0.093	Pro
IL18	0.45	0.038	Pro
HIF1A	0.48	0.097	Pro

FIGURE 5. T cell infiltration rates and immunity-related gene expression in GBM tumors treated with TTFields therapy. (**A** and **B**) GBM tumor samples were obtained from four patients before and after treatment with TTFields combined with standard chemoradiation. Samples were embedded in paraffin blocks, sliced, and stained by H&E for nuclear visualization and by IHC for CD3, CD4, and CD8. (A) Cells were counted in 4–6 representative fields from each slide at original magnification ×20 and cell count per millimeter squared was calculated. Graphs show mean cell densities (cells per millimeter squared) of $CD3^+$, $CD4^+$, and $CD8^+$ cells for each patient before and after therapy. (B) Representative IHC images of tissue section from patient 4*. Positive cells are stained brown. (**C**) GBM samples were obtained before and after a treatment from six patients treated by TTFields + chemoradiation and six patients treated by standard chemoradiation only (controls). Gene expression analysis was performed by RNA-Seq. The negative binomial generalized linear model was used to analyze expression following treatment. Net treatment effect was calculated per patient by subtracting a gene's *(Figure legend continues)*

assay also represents the first time that CAR-T cell functionality was examined in the context of TTFields.

A differential response of tumor cell lines to various TTFields frequencies has been previously demonstrated (18). Matching optimal frequencies to specific cancers is a cornerstone of TTFields clinical use, as demonstrated by the recent approval of TTFields treatment for mesothelioma employing 150 kHz frequency rather than 200 kHz as used for GBM. An in-depth study of T cell functionality under the entire clinically relevant frequency spectrum of TTFields is not within the scope of this study. Notwithstanding, we did test how the phenomena observed in 200 kHz apply to additional frequencies in the range of 100–500 kHz (Supplemental Fig. 3A, 3B). The strongest negative effects on proliferating T cells were observed at 200 kHz followed by 300 kHz. TTFields' frequencies of 100 kHz and 150 kHz showed no negative effects on T cell viability or functionality.

Although there is no evidence of a reduction in T cell counts within tumors or in peripheral blood in numerous TTFields preclinical or clinical studies, the inhibitory impact of TTFields on the capacity of intratumoral T cell to proliferate could be of concern. It is not yet clear if, and to what extent, intratumoral TASTs proliferate within GBM and other solid malignancies. Expanded TCRs clonotypes found among TIL populations in GBM and other tumors indicate that proliferation of TASTs does occur (37) but not where it had occurred. Murine studies have yielded conflicting findings, some having shown that brain-Ag–specific T cells do not proliferate within the brain (38), whereas others demonstrating that the brain microenvironment may support in situ proliferation under some circumstances (39).

Of note is that brain- or tumor-specific T cell priming, and proliferation were shown to occur in the meningeal lymphatics (40) and within the deep cervical lymph nodes (6), found outside the TTFields-affected area. The case of mesothelioma, in which TTFields have been approved, or lung and liver cancers, in which TTFields are currently in advanced clinical phases, might be different. In these cases, some tumor-draining lymph nodes may be found within the treated field. Notwithstanding, the data presented in Supplemental Fig. 3 demonstrate that 150 kHz (the frequency used to treat said tumors) had no negative effects on the number, functionality, or viability of T cells.

Importantly, several studies have indicated that only peripheral T cells, and not intratumoral ones, bear sustained proliferative capabilities, and that T cell activation and proliferation must occur within peripheral lymphoid organs to achieve tumor eradication (30, 41). A recent study provided evidence of clonotypic expansion of effector-like T cells in four different tumor types, both within the tumor as well as in adjacent normal tissue and within peripheral blood (42). Patients exhibiting a wide clonotypic expansion pattern were those most likely to respond to anti-PDL1 therapy. The authors suggested that tumor-Ag–specific TILs are replenished by nonexhausted T cells arriving from outside the tumor. If this applies also to brain tumors, it is reasonable to expect that the effect of TTFields on the proliferation of intratumoral T cells should have minor clinically meaningful implications. The effects that TTFields were found to have on proliferating T cells suggest that appropriate consideration of TTFields parameters (i.e., field frequency, intensity, and administration protocols) should be taken to balance between maximizing tumor cell killing and minimizing the disruption of T cell function.

In recent years there have been a surge of scientific data demonstrating that beyond their documented immunosuppressive effects, both temozolomide (43) and irradiation (44) can exert potent immunostimulatory effects either alone or in combination (43). These effects are mediated by temozolomide through the enhancement of mortal levels of autophagy (43) and by irradiation through the induction of ICD and by the production of type I IFNs, downstream of CGAS signaling driven by cytosolic dsDNA (44).

Whereas the ICD-related effects of TTFields were demonstrated elsewhere (12–14), to our knowledge, our study is the first to report comparison of patients' RNA-Seq data obtained from pre-postchemoradiation treatment versus prepost-TTFields + chemoradiation treatment. This comparison enables to dissect the relative immune contribution of TTFields. Our transcriptional analysis focused on a large set of immune-related genes and demonstrated a shift from a protumoral Th_2 or a Th_{17}-related profile, previously associated with unfavorable prognosis in GBM (45), to a more antitumoral Th_1-associated profile (46). Regarding T cells infiltration to tumors, The IHC data from four patients that was complemented by RNA-Seq data from 12 additional patients, demonstrated that TTFields do not preclude nor reduce the accumulation of T cells within GBMs.

The in vitro mechanistic data in this study focused on evaluating potentially deleterious effects of TTFields on the T cell level, whereas the clinical part demonstrated potentially beneficial effects of TTFields on the patient level. TTFields' potential to clinically synergize with immunotherapy is beyond the scope of this work and is currently addressed by several clinical trials. However, TTFields ability to operate alongside, and in some cases, synergize with antitumoral responses has been demonstrated when it was shown to enhance T cell infiltration in various tumor models (11, 14). Voloshin et al. have recently provided direct evidence of TTFields inducing ICD in multiple murine tumor cell lines. The authors demonstrated synergism in vivo in two murine tumor models between treatment with a PD1 inhibitor and TTFields application (14).

Correlative clinical data from GBM patients revealed that the survival benefit from TTFields correlates with higher blood T cell counts and with low or no administration of dexamethasone (15). Although these data do not reveal cause and effect, they concur with both the mouse in vivo data (14) and with our human data, substantiating a possible contribution of an intact immune compartment to the clinical benefits provided by TTFields.

Given our findings and the nature of TTFields, several approaches for combining this modality with immunotherapy are conceivable. Combining TTFields with CPIs may couple tumor cell death by ICD (14) (TTFields) with attenuation of T cell exhaustion (e.g., PD1), or expanded breadth of responding T cells (CTLA4). This approach bears some similarity to the combination of CPIs with ICD-inducing oncolytic viruses (47) or radiotherapy (48, 49).

expression level at pretreatment from its expression level posttreatment. Differences between treatments were calculated as fold change between average net effect in the TTFields group versus control group. A list of 712 immune activity-related genes was evaluated. A significant effect of TTFields on expression was defined as an average fold change of either >2 or <0.5, with $p < 0.1$. (C) A list of the genes exhibiting significantly altered expression. Each gene was designated as having primarily pro-/anti-/mixed-tumoral activity based on literature review.

The first clinical studies combining treatment with alternating electrical-fields and various immune-modulating treatments are already underway. As preclinical and clinical data demonstrate the significant overall antitumor immunity function of TTFields, the mechanistic and clinical data provided in this study strengthens these clinical studies' rationale and provides important knowledge required to interpret their results.

Acknowledgments

We thank Dr. Moshe Giladi, and Dr. Tali Voloshin for inovitro technical support and for fruitful scientific exchange.

Disclosures

Z.R. is serving as a consultant for and holding stock options in Novocure. The other authors have no financial conflicts of interest.

References

1. Kirson, E. D., Z. Gurvich, R. Schneiderman, E. Dekel, A. Itzhaki, Y. Wasserman, R. Schatzberger, and Y. Palti. 2004. Disruption of cancer cell replication by alternating electric fields. *Cancer Res.* 64: 3288–3295.
2. Wang, Y., M. Pandey, and M. T. Ballo. 2019. Integration of tumor-treating fields into the multidisciplinary management of patients with solid malignancies. *Oncologist* 24: e1426–e1436.
3. Mittal, S., N. V. Klinger, S. K. Michelhaugh, G. R. Barger, S. C. Pannullo, and C. Juhasz. 2017. Alternating electric tumor treating fields for treatment of glioblastoma: rationale, preclinical, and clinical studies. *J. Neurosurg.* 128: 414–421.
4. Ceresoli, G. L., J. G. Aerts, R. Dziadziuszko, R. Ramlau, S. Cedres, J. P. van Meerbeeck, M. Mencoboni, D. Planchard, A. Chella, L. Crinò, et al. 2019. Tumour treating fields in combination with pemetrexed and cisplatin or carboplatin as first-line treatment for unresectable malignant pleural mesothelioma (STELLAR): a multicentre, single-arm phase 2 trial. *Lancet Oncol.* 20: 1702–1709.
5. Stupp, R., A. Idbaih, D. M. Steinberg, W. Read, S. Toms, G. Barnett, G. Nicholas, C.-Y. Kim, K. Fink, A. Salmaggi, et al. 2016. LTBK-01: prospective multi-center phase III trial of tumor treating fields together with temozolomide compared with temozolomide alone in patients with newly diagnosed glioblastoma. *Neuro Oncol.* 18: i1 (Abstr.).
6. Sampson, J. H., M. V. Maus, and C. H. June. 2017. Immunotherapy for brain tumors. *J. Clin. Oncol.* 35: 2450–2456.
7. Gibney, G. T., L. M. Weiner, and M. B. Atkins. 2016. Predictive biomarkers for checkpoint inhibitor-based immunotherapy. *Lancet Oncol.* 17: e542–e551.
8. Melero, I., D. M. Berman, M. A. Aznar, A. J. Korman, J. L. Pérez Gracia, and J. Haanen. 2015. Evolving synergistic combinations of targeted immunotherapies to combat cancer. *Nat. Rev. Cancer* 15: 457–472.
9. Lim, M., Y. Xia, C. Bettegowda, and M. Weller. 2018. Current state of immunotherapy for glioblastoma. *Nat. Rev. Clin. Oncol.* 15: 422–442.
10. Sharma, P., and J. P. Allison. 2015. The future of immune checkpoint therapy. *Science* 348: 56–61.
11. Kirson, E. D., M. Giladi, Z. Gurvich, A. Itzhaki, D. Mordechovich, R. S. Schneiderman, Y. Wasserman, B. Ryffel, D. Goldsher, and Y. Palti. 2009. Alternating electric fields (TTFields) inhibit metastatic spread of solid tumors to the lungs. *Clin. Exp. Metastasis* 26: 633–640.
12. Voloshin T., S. Davidi, Y. Porat, A. Shteingauz, M. Munster, N. Kaynan, R. Schneiderman, C. T. Brami, E. Zeevi, K. Gotlib, et al. 2019. Immunomodulatory effect of tumor treating fields (TTFields) results in enhanced antitumor efficacy when combined with anti-PD-1 therapy in mouse model of lung cancer. *Int. J. Radiat. Oncol. Biol. Phys.* 104: 237.
13. Swanson, K. D., E. Lok, and E. T. Wong. 2016. An overview of alternating electric fields therapy (NovoTTF Therapy) for the treatment of malignant glioma. *Curr. Neurol. Neurosci. Rep.* 16: 8.
14. Voloshin T., N. Kaynan, S. Davidi, Y. Porat, A. Shteingauz, R. S. Schneiderman, E. Zeevi, M. Munster, R. Blat, and C. T. Brami, et al. 2020. Tumor-treating fields (TTFields) induce immunogenic cell death resulting in enhanced antitumor efficacy when combined with anti-PD-1 therapy. *Cancer Immunol. Immunother.* 69: 1191–1204.
15. Wong, E. T., E. Lok, S. Gautam, and K. D. Swanson. 2015. Dexamethasone exerts profound immunologic interference on treatment efficacy for recurrent glioblastoma. [Published erratum appears in 2015 *Br. J. Cancer* 113: 1642]. *Br. J. Cancer* 113: 232–241.
16. Volovitz, I., N. Shapira, H. Ezer, A. Gafni, M. Lustgarten, T. Alter, I. Ben-Horin, O. Barzilai, T. Shahar, A. Kanner, et al. 2016. A non-aggressive, highly efficient, enzymatic method for dissociation of human brain-tumors and brain-tissues to viable single-cells. *BMC Neurosci.* 17: 30.
17. Globerson-Levin, A., T. Waks, and Z. Eshhar. 2014. Elimination of progressive mammary cancer by repeated administrations of chimeric antigen receptor-modified T cells. *Mol. Ther.* 22: 1029–1038.
18. Porat, Y., M. Giladi, R. S. Schneiderman, R. Blat, A. Shteingauz, E. Zeevi, M. Munster, T. Voloshin, N. Kaynan, O. Tal, et al. 2017. Determining the optimal inhibitory frequency for cancerous cells using tumor treating fields (TTFields). *J. Vis. Exp.* 123: 55820.
19. Kirson, E. D., V. Dbalý, F. Tovarys, J. Vymazal, J. F. Soustiel, A. Itzhaki, D. Mordechovich, S. Steinberg-Shapira, Z. Gurvich, R. Schneiderman, et al. 2007. Alternating electric fields arrest cell proliferation in animal tumor models and human brain tumors. *Proc. Natl. Acad. Sci. USA* 104: 10152–10157.
20. Lamoreaux, L., M. Roederer, and R. Koup. 2006. Intracellular cytokine optimization and standard operating procedure. *Nat. Protoc.* 1: 1507–1516.
21. Love, M. I., W. Huber, and S. Anders. 2014. Moderated estimation of fold change and dispersion for RNA-seq data with DESeq2. *Genome Biol.* 15: 550.
22. Burkhardt, J. K., E. Carrizosa, and M. H. Shaffer. 2008. The actin cytoskeleton in T cell activation. *Annu. Rev. Immunol.* 26: 233–259.
23. Hottinger, A. F., P. Pacheco, and R. Stupp. 2016. Tumor treating fields: a novel treatment modality and its use in brain tumors. *Neuro-oncol.* 18: 1338–1349.
24. Betts, M. R., J. M. Brenchley, D. A. Price, S. C. De Rosa, D. C. Douek, M. Roederer, and R. A. Koup. 2003. Sensitive and viable identification of antigen-specific CD8+ T cells by a flow cytometric assay for degranulation. *J. Immunol. Methods* 281: 65–78.
25. Betts, M. R., M. C. Nason, S. M. West, S. C. De Rosa, S. A. Migueles, J. Abraham, M. M. Lederman, J. M. Benito, P. A. Goepfert, M. Connors, et al. 2006. HIV nonprogressors preferentially maintain highly functional HIV-specific CD8+ T cells. *Blood* 107: 4781–4789.
26. Restifo, N. P., M. E. Dudley, and S. A. Rosenberg. 2012. Adoptive immunotherapy for cancer: harnessing the T cell response. *Nat. Rev. Immunol.* 12: 269–281.
27. Lin, L., J. Couturier, X. Yu, M. A. Medina, C. A. Kozinetz, and D. E. Lewis. 2014. Granzyme B secretion by human memory CD4 T cells is less strictly regulated compared to memory CD8 T cells. *BMC Immunol.* 15: 36.
28. Terahara, K., H. Ishii, T. Nomura, N. Takahashi, A. Takeda, T. Shiino, Y. Tsunetsugu-Yokota, and T. Matano. 2014. Vaccine-induced CD107a+ CD4+ T cells are resistant to depletion following AIDS virus infection. *J. Virol.* 88: 14232–14240.
29. Mahnke, Y. D., T. M. Brodie, F. Sallusto, M. Roederer, and E. Lugli. 2013. The who's who of T-cell differentiation: human memory T-cell subsets. *Eur. J. Immunol.* 43: 2797–2809.
30. Spitzer M. H., Y. Carmi, N. E. Reticker-Flynn, S. S. Kwek, D. Madhireddy, M. M. Martins, P. F. Gherardini, T. R. Prestwood, J. Chabon, S. C. Bendall, et al. 2017. Systemic immunity is required for effective cancer immunotherapy. *Cell.* 168: 487–502.e15.
31. Ahmadzadeh, M., L. A. Johnson, B. Heemskerk, J. R. Wunderlich, M. E. Dudley, D. E. White, and S. A. Rosenberg. 2009. Tumor antigen-specific CD8 T cells infiltrating the tumor express high levels of PD-1 and are functionally impaired. *Blood* 114: 1537–1544.
32. Donia, M., J. W. Kjeldsen, R. Andersen, M. C. W. Westergaard, V. Bianchi, M. Legut, M. Attaf, B. Szomolay, S. Ott, G. Dolton, et al. 2017. PD-1^{+} polyfunctional T cells dominate the periphery after tumor-infiltrating lymphocyte therapy for cancer. *Clin. Cancer Res.* 23: 5779–5788.
33. de la Roche, M., Y. Asano, and G. M. Griffiths. 2016. Origins of the cytolytic synapse. *Nat. Rev. Immunol.* 16: 421–432.
34. Ramos, C. A., H. E. Heslop, and M. K. Brenner. 2016. CAR-T cell therapy for lymphoma. *Annu. Rev. Med.* 67: 165–183.
35. O'Rourke, D. M., M. P. Nasrallah, A. Desai, J. J. Melenhorst, K. Mansfield, J. J. D. Morrissette, M. Martinez-Lage, S. Brem, E. Maloney, A. Shen, et al. 2017. A single dose of peripherally infused EGFRvIII-directed CAR T cells mediates antigen loss and induces adaptive resistance in patients with recurrent glioblastoma. *Sci. Transl. Med.* 9: eaaa0984.
36. Silginer, M., M. Weller, and P. Roth. 2018. IMMU-53. Impact of tumor-treating fields (TTFIELDS) on the immunogenicity of glioma cells. *Neuro Oncol.* 20: vi133.
37. Sims, J. S., B. Grinshpun, Y. Feng, T. H. Ung, J. A. Neira, J. L. Samanamud, P. Canoll, Y. Shen, P. A. Sims, and J. N. Bruce. 2016. Diversity and divergence of the glioma-infiltrating T-cell receptor repertoire. *Proc. Natl. Acad. Sci. USA* 113: E3529–E3537.
38. Aloisi, F., F. Ria, and L. Adorini. 2000. Regulation of T-cell responses by CNS antigen-presenting cells: different roles for microglia and astrocytes. *Immunol. Today* 21: 141–147.
39. Masson, F., T. Calzascia, W. Di Berardino-Besson, N. de Tribolet, P. Y. Dietrich, and P. R. Walker. 2007. Brain microenvironment promotes the final functional maturation of tumor-specific effector CD8+ T cells. *J. Immunol.* 179: 845–853.
40. Schläger, C., H. Körner, M. Krueger, S. Vidoli, M. Haberl, D. Mielke, E. Brylla, T. Issekutz, C. Cabañas, P. J. Nelson, et al. 2016. Effector T-cell trafficking between the leptomeninges and the cerebrospinal fluid. *Nature* 530: 349–353.
41. Carmi, Y., M. H. Spitzer, I. L. Linde, B. M. Burt, T. R. Prestwood, N. Perlman, M. G. Davidson, J. A. Kenkel, E. Segal, G. V. Pusapati, et al. 2015. Allogeneic IgG combined with dendritic cell stimuli induce antitumour T-cell immunity. *Nature* 521: 99–104.
42. Wu, T. D., S. Madireddi, P. E. de Almeida, R. Banchereau, Y.-J. J. Chen, A. S. Chitre, E. Y. Chiang, H. Iftikhar, W. E. O'Gorman, A. Au-Yeung, et al. 2020. Peripheral T cell expansion predicts tumour infiltration and clinical response. *Nature* 579: 274–278.
43. Liikanen, I., L. Ahtiainen, M. L. Hirvinen, S. Bramante, V. Cerullo, P. Nokisalmi, O. Hemminki, I. Diaconu, S. Pesonen, A. Koski, et al. 2013. Oncolytic adenovirus with temozolomide induces autophagy and antitumor immune responses in cancer patients. *Mol. Ther.* 21: 1212–1223.
44. Galluzzi, L., I. Vitale, S. Warren, S. Adjemian, P. Agostinis, A. B. Martinez, T. A. Chan, G. Coukos, S. Demaria, E. Deutsch, et al. 2020. Consensus guidelines for the definition, detection and interpretation of immunogenic cell death.

[Published erratum appears in 2020 *J. Immunother. Cancer* 8: e000337corr1]. *J. Immunother. Cancer* 8: e000337.
45. Madkouri, R., C. G. Kaderbhai, A. Bertaut, C. Truntzer, J. Vincent, M. H. Aubriot-Lorton, W. Farah, E. Limagne, S. Ladoire, R. Boidot, et al. 2017. Immune classifications with cytotoxic $CD8^+$ and Th17 infiltrates are predictors of clinical prognosis in glioblastoma. *OncoImmunology* 6: e1321186.
46. Fridman, W. H., L. Zitvogel, C. Sautès-Fridman, and G. Kroemer. 2017. The immune contexture in cancer prognosis and treatment. *Nat. Rev. Clin. Oncol.* 14: 717–734.
47. Saha, D., R. L. Martuza, and S. D. Rabkin. 2017. Macrophage polarization contributes to glioblastoma eradication by combination immunovirotherapy and immune checkpoint blockade. *Cancer Cell* 32: 253–267.e5.
48. Deng, L., H. Liang, B. Burnette, M. Beckett, T. Darga, R. R. Weichselbaum, and Y. X. Fu. 2014. Irradiation and anti-PD-L1 treatment synergistically promote antitumor immunity in mice. *J. Clin. Invest.* 124: 687–695.
49. Wu, C. T., W. C. Chen, Y. H. Chang, W. Y. Lin, and M. F. Chen. 2016. The role of PD-L1 in the radiation response and clinical outcome for bladder cancer. *Sci. Rep.* 6: 19740.

Supplementary Table STI

Summary of patient data (figures 5 and S4)

Assay	Treatment	Patient no.	Sex	Age (years)	Days between ops
IHC	Chemo + TTFields	2*	M	59	310
		4*	F	58	178
		5*	M	57	544
		6*	M	46	768

Assay	Treatment	Patient no.	Sex	Age (years)	TTF (weeks)	DFS
NGS	Chemo + TTFields	1	F	32	95	614
		2	F	59	95	311
		3	M	57	95	514
		4	M	58	8	176
		5	F	61	3	427
		6	M	47	7	88d
	Chemo only	8	F	62	-	806
		9	F	57	-	281
		11	M	59	-	548
		13	M	61	-	222
		16	F	59	-	634
		17	M	52	-	544

* Pathological findings reported WHO grade 4 glioblastoma or gliosarcoma for all patients.
* Adjuvant therapy (Chemo) for all patients was performed according to the STUPP protocol.
* Extents of all operations was gross total resection.

Op – operation; DFS – disease free survival; IHC – immunohistochemistry; NGS – RNAseq analysis

Table ST1: Details of patient samples used to generate the data presented in main figure 5.

Supplementary fig. S1

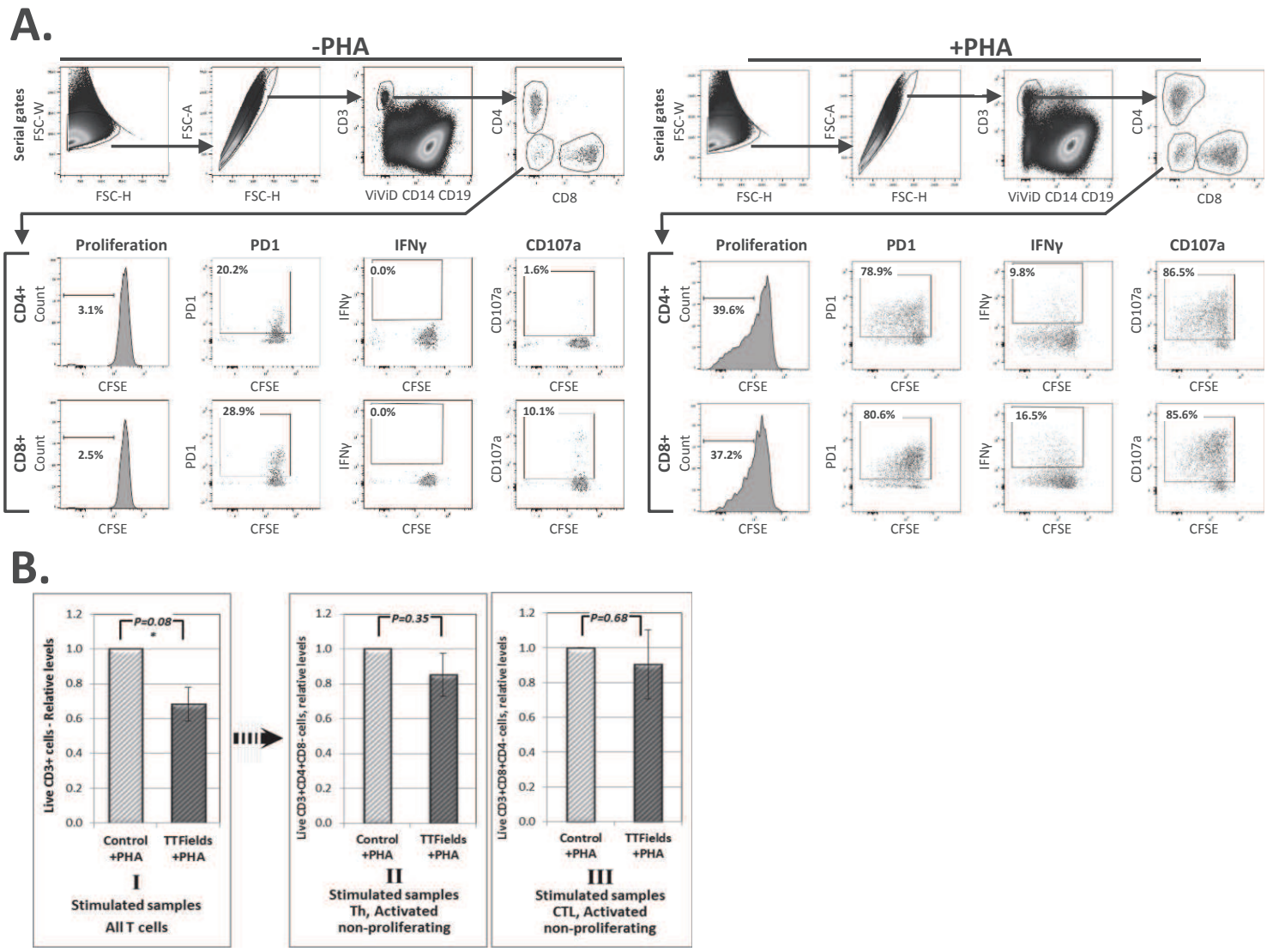

Fig. S1: Effects of TTFields on activation of GBM TILs. (A) Representative gating strategy for PHA-stimulated and unstimulated GBM TIL culture. PB samples were used for gate placement (not shown). Gating strategy consisted of singlet discrimination (x2) → gating of live T cells as $CD3^{+}ViViD^{low}CD14^{-}CD19^{-}$ → division into $CD4^{+}8^{-}$ Th and $CD8^{+}4^{-}$ CTL. Each T cell subset was then evaluated for surface expression of PD-1 and CD107a, for CFSE dilution and for intracellular expression of IFNγ. Gating of Tγδ cells using $CD3^{+}CD4^{-}CD8^{-}$ identified a lower percentage of Tγδ cells than in PB and thus was not used. **(B)** Analysis of T cell viability in stimulated cells. (I) The fraction of live T cells in each PHA-stimulated TIL sample. Data from 3 repeats was normalized by setting the value of the control+PHA sample to 1. Polyfunctional analysis was used to enumerate the cells that were negative for proliferation but positive for at least one other activation parameter. Graphs represent the relative fractions of these cells within the $CD4^{+}$ (II) and the $CD8^{+}$ (III) T cell subsets. Results show no significant decline in the number of activated T cells which did not attempt to proliferate. The significant reduction noted in (I) thus consists mostly of the activated T cells which attempted to proliferate.

Supplementary fig. S2

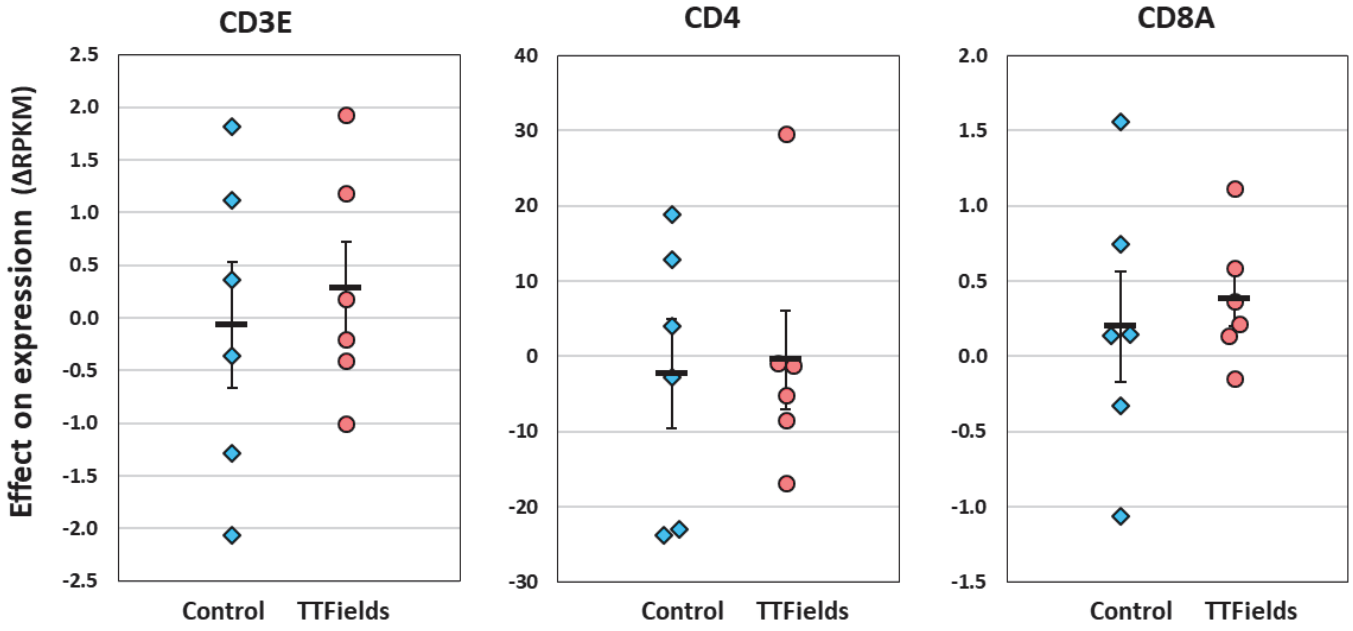

Fig. S2: Gene expression analysis of CD3, CD4 and CD8 in GBM tumors following TTFields therapy. Samples of GBM resections were taken from before and after a treatment course by standard chemoradiation (i.e. Stupp protocol, control) versus approved TTFields protocol (Optune + chemoradiation). Total RNA was purified and sequenced by NGS.
RNAseq quality control check was performed using FastQC v0.11.5. Reads were trimmed using Trimmomatic v0.36 (for removing sequencing adapters) . Reads were mapped to *Homo sapiens* genome (Grch38) using STAR read aligner v2.4.2a (default parameters) . Counting proceeded over genes annotated in Ensembl release 83, using featureCounts . Read counting, normalization and conversion to RPKM were performed using edgeR v3.4.1 v3.4.1.
Statistic analysis was carried out using the negative binomial generalized linear model. Charts show the difference in RPKM between post- and per-treatment expression for each patient by group (12 patients total) using DESeq2. Group averages are shown as a black line with standard error bars.

Supplementary fig. S3

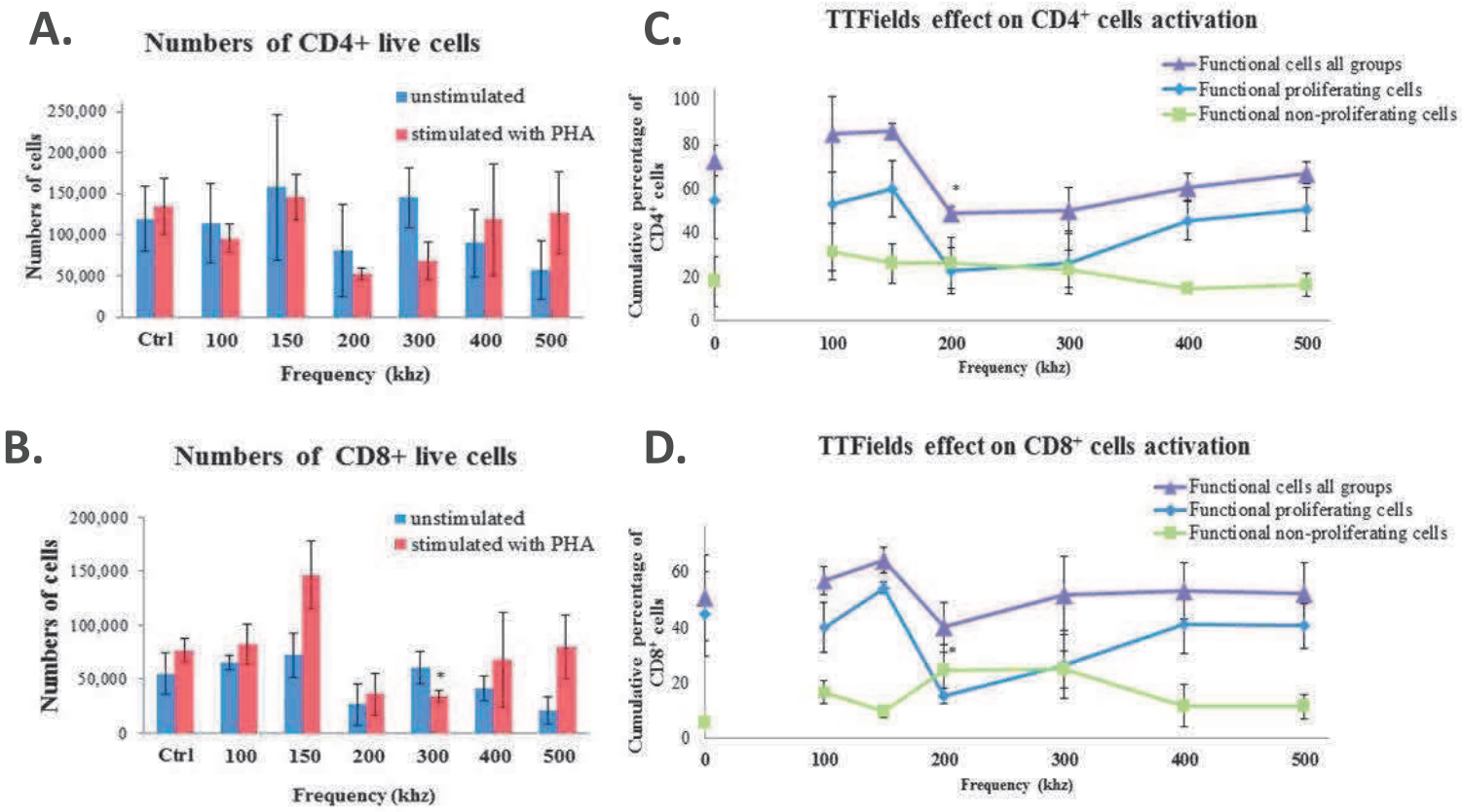

Figure S3. Effects of variable TTFields frequencies on the viability and polyfunctionality of CD4⁺ and CD8⁺ T cells. Equal numbers of healthy donor PBMC were cultured for 3 days under TTFields or standard culture conditions, with or without phytohemaglutinin (PHA) serving as a mitogen/superantigen. The cells were then collected and adjusted to 350ul, then read for 2.5 minutes of FACS CANTO-II drawing equal sample volumes per minute/sample – see methods.

(A+B) The numbers of viable PHA-unstimulated CD4 or CD8 T cells (blue bars in panels A, B respectively) cultured at different frequencies were compared to the TTFields-untreated PHA-unstimulated control (frequency 0 kHz); no significant changes were found. Reduction in the numbers of viable PHA-stimulated CD4 (A) or CD8 (B) T cells versus matched TTFields-untreated, PHA-stimulated controls, was found at 200kHz and 300 kHz. These results reiterate those in figure 1B for 200KHz. **(C,D)** The same cultures were also evaluated for four concurrent T cell functions: proliferation (CFSE dilution), cytotoxic degranulation (CD107 surface expression), IFNγ secretion and PD1 upregulation (activation/exhaustion) – see methods. Net functional/polyfunctional T cell fractions were calculated by deducting the fraction of functional/polyfunctional cells in the PHA-unstimulated sample from the matching category in the PHA-stimulated one. The polyfunctionality data demonstrates a reduction in the fraction of proliferating, 1-4 function positive T cells at 200 and 300 kHz ("functional proliferating cells" – blue line); this effect was observed on both CD4+ ($P<0.05$) (C) and on CD8+ T cells (NS), and, to some extent in the 300 kHz frequency (NS). The decreases observed in the fraction of the functional and proliferating T cells occurred with a concurrent increase in the fraction of functional T cells which did not proliferate ("functional non-proliferating cells" - green line); this effect was observed in the CD8+ T cells at 200 kHz ($P<0.05$) and at 300kHz (NS). These shifts from functional proliferating groups to functional non-proliferating groups was mostly found in populations that differed from each other in one function – proliferation, reiterating the results shown in figure 3B evaluating the similar effects at 200kHz. Statistics: t-test $P<0.05$, assays were repeated 3 times with similar results; 100 and 150KHz - 2 repeats.